On the apparent coupling of neutral hydrogen and dark matter in spiral galaxies

Hoekstra, H.; van Albada, T. S.; Sancisi, R.

Published in:
Monthly Notices of the Royal Astronomical Society

DOI:
10.1046/j.1365-8711.2001.04214.x

Mon. Not. R. Astron. Soc. **323**, 453–459 (2001)

On the apparent coupling of neutral hydrogen and dark matter in spiral galaxies

H. Hoekstra,[1★†] T. S. van Albada[1] and R. Sancisi[1,2]
[1]*Kapteyn Astronomical Institute, University of Groningen, Postbus 800, 9700 AV Groningen, the Netherlands*
[2]*Osservatorio Astronomico, Via Ranzani 1, I-40127 Bologna, Italy*

Accepted 2000 November 10. Received 2000 October 13; in original form 2000 September 8

ABSTRACT

We have studied a mass model for spiral galaxies in which the dark matter surface density is a scaled version of the observed H I surface density. Applying this mass model to a sample of 24 spiral galaxies with reliable rotation curves, one obtains good fits for most galaxies. The scaling factors cluster around 7, after correction for the presence of primordial helium. For several cases, however, different, often larger, values are found. For galaxies that cannot be fitted well, the discrepancy occurs at large radii and results from a fairly rapid decline of the H I surface density in the outermost regions. Because of such imperfections and in view of possible selection effects, it is not possible to conclude here that there is a real coupling between H I and dark matter in spiral galaxies.

Key words: methods: analytical – galaxies: haloes – galaxies: kinematics and dynamics – galaxies: spiral – cosmology: theory – dark matter.

1 INTRODUCTION

The first indications that spiral galaxies are surrounded by unseen matter date to the early 1970s (Freeman 1970; Shostak 1973; Roberts & Whitehurst 1975). Later 21-cm line studies, especially those of Bosma (1978, 1981) and Begeman (1987), have all confirmed this discovery. Dark matter manifests itself already in the outer(most) parts of the luminous body of spiral galaxies (Rubin, Thonnard & Ford 1978; Kent 1986), but its main signature is the general flatness of rotation curves well outside the optical radius.

Bosma (1978, 1981) noted a curious result for the galaxies in his sample: the total surface density of matter needed to explain the observed rotation curve in the outer region, i.e. outside the optical radius, was roughly proportional to the surface density of neutral hydrogen. Later work has shown that this proportionality holds not only for the high surface brightness (HSB) galaxies studied by Bosma, but also for dwarf galaxies (Carignan 1985a; Carignan & Puche 1990; Jobin & Carignan 1990).

These results, and other considerations, have led Pfenniger, Combes & Martinet (1994a,b) to the hypothesis that the dark matter surrounding spiral galaxies consists of cold gas, mainly in the form of molecular hydrogen. The spatial distribution of this cold gas should be similar to that of the observed neutral hydrogen.

As the contribution of luminous matter to the total mass density is negligible in the outer parts (under the assumption that the mass-to-light ratio of the luminous matter is independent of radius), Bosma's relationship is equivalent to a proportionality between dark matter and neutral hydrogen.

This apparent coupling of dark matter and neutral hydrogen deserves closer scrutiny, because it seems at odds with the current view that dark haloes are triaxial (but not extremely flattened) and that they consist of non-baryonic material. Rather, this coupling suggests possible support for the hypothesis put forth by Pfenniger et al. (1994a).

Several questions should be considered: (i) How tight is this correlation between the surface densities of H I and dark matter for the galaxies with the best available data? (ii) To what extent does the relation depend on the use of the so-called maximum disc assumption? (iii) Does the relation also hold for the low surface brightness (LSB) galaxies?

In this paper we investigate the apparent coupling of dark matter and neutral hydrogen for a sample of 24 spiral galaxies with good rotation curves. The sample contains both HSB and dwarf galaxies. Unfortunately, the quality of the rotation curves for LSB galaxies is still rather poor, and we have decided not to include those galaxies in the present discussion.

We wish to stress at the outset that there is a potentially powerful selection effect that may cause a relationship between the surface densities of H I and dark matter for the galaxies in our sample. This is because the H I surface density distributions of the galaxies in our sample have the common characteristic that the highest values in the inner regions, as well as the lowest values in the outer regions, are similar from galaxy to galaxy (the latter being linked to the sensitivity reached in the observations). As a result, a large radial extent implies a large radial scalelength of

★Present address: CITA and Astronomy Department, University of Toronto, 60 St. George Street, M55 3H8 Toronto, Canada.
†E-mail: hoekstra@cita.utoronto.ca

H I, and vice versa. In Section 5 we discuss how this can lead to a proportionality between dark matter and H I.

2 MASS MODEL

To study the mass distribution, and in particular the apparent coupling between the dark matter and H I, we use axisymmetric distributions of matter containing three components. These are used to model the derived rotation curves. The various components of the mass model are as follows.

(i) *Stars*: The stars are distributed in a disc. If present, we also include a bulge component. The radial surface density profiles of the stellar components are estimated using luminosity profiles from the literature, assuming a mass-to-light ratio independent of radius. We further assume that the stellar disc has an exponential vertical density profile, with a scaleheight that is one-fifth of the optical disc scalelength (van der Kruit & Searle 1981a,b).

(ii) *Gas*: We use the observed radial surface density distribution of H I and we assume that the vertical distribution mimics that of the stars. In reality most of the neutral hydrogen lies in a thin disc, but our results are not sensitive to the detailed z distribution because in the inner regions (where the thick disc description for H I does not hold) the contribution of H I to the gravitational field can be safely neglected. Apart from neutral hydrogen, detectable through the 21-cm line, galaxies contain molecular gas. We assume that the bulk of this molecular gas follows the surface density profile of the stellar component. In this way the presence of molecular gas is taken into account in the value of the mass-to-light ratio of the stellar component.

(iii) *Dark matter*: Usually a spherical halo is used to describe the density distribution of the dark matter. If the dark matter and neutral hydrogen are indeed coupled, as Pfenniger et al. (1994a) argue, it is reasonable to assume that their spatial distributions are similar. In this paper we therefore assume that the surface density of dark matter is proportional to the observed surface density of neutral hydrogen. The vertical scaleheight of the dark matter, like that of H I, is taken equal to that of the stars. For the discussion in this paper the choice of the scaleheight is fairly arbitrary because the changes in calculated rotation velocities, given a surface density profile, are small when the scaleheight is varied. But the derived total masses do depend on scaleheight.

The mass model can be fitted to the observations in two ways: one can fit the model rotation curve to the observed one; or one can compare the total surface density, calculated from the rotation curve, to the measured surface densities of stars and H I. We prefer to fit the circular velocities calculated from the mass model to the observed rotation curves. To do so, we compute the rotation velocity of a disc using (Cuddeford 1993):

$$V_{\rm c}^2(R) = 2\pi GR\int_0^\infty {\rm d}k\,\frac{S(k)}{1+k\epsilon}kJ_1(kR), \qquad (1)$$

where $J_\nu(x)$ is the Bessel function of order ν and $S(k)$ is given by

$$S(k) = \int_0^\infty {\rm d}R'\Sigma(R')R'J_0(kR'). \qquad (2)$$

In these equations $\Sigma(R)$ is the surface density of the disc as a function of radius R, and ϵ is the scaleheight of the disc, assuming a density profile given by $\rho(x,y,z) = \Sigma(R)\,{\rm e}^{-z/|\epsilon|}$.

Equation (1) requires that the surface density is known out to infinity. This can only be achieved through extrapolation, for which we assumed an exponential law. At large radii the surface densities are low, thus giving rise to minor contributions to the integral. Finally, the model rotation curve is calculated by adding the circular velocities, calculated for the different components, in quadrature:

$$V_{\rm tot}^2 = \left(\frac{\Sigma_{\rm dark}}{\Sigma_{\rm H\,I}}+1\right)V_{\rm H\,I}^2 + \left(\frac{M}{L_B}\right)_{\rm bulge}V_{\rm bulge}^2 + \left(\frac{M}{L_B}\right)_{\rm disc}V_{\rm disc}^2, \qquad (3)$$

where $\Sigma_{\rm dark}$ denotes the surface density of the dark matter component and $\Sigma_{\rm H\,I}$ is the surface density of the H I disc.

In making the fits we have three free parameters at our disposal: $\Sigma_{\rm dark}/\Sigma_{\rm H\,I}$, $(M/L_B)_{\rm bulge}$ and $(M/L_B)_{\rm disc}$. For late-type galaxies, which show no clear signs of a bulge, we omitted the (spherical) bulge contribution. The fits were done by eye, in such a way that the model rotation curve explained the observed rotation curve as far out as possible.

Table 1. Basic properties of the selected galaxies.

Name	Type	Distance (Mpc)	$M_B^{b,i}$ (mag)	$V_{\rm max}$ (km s^{-1})	Ref.
(1)	(2)	(3)	(4)	(5)	(6)
DDO 154	Irr	4.0	−13.8	48	1, 2
DDO 168	Irr	3.5	−15.2	55	3
DDO 170	Sm	12.0	−14.5	66	4
NGC 55	Sm	1.6	−18.6	87	5
NGC 247	Sd	2.5	−18.0	108	6, 7
NGC 300	Sd	1.8	−17.8	97	8, 7
NGC 801	Sc	79.2	−21.7	238	3, 10
NGC 1560	Sd	3.0	−15.9	79	12
NGC 2403	Scd	3.3	−19.3	136	13, 14, 23
NGC 2841	Sb	18.0	−21.7	326	13, 14
NGC 2903	Sbc	6.4	−20.0	216	13, 14
NGC 2998	Sc	67.4	−21.9	214	3, 10
NGC 3109	Sm	1.7	−16.8	67	14, 15
NGC 3198	Sc	9.4	−19.4	157	14, 16
NGC 5033	Sbc	11.9	−20.2	225	10, 13
NGC 5371	Sb	34.8	−21.7	242	13, 20
NGC 5533	Sab	55.8	−21.4	302	3, 9, 18
NGC 5585	Sd	6.2	−17.5	92	19
NGC 6503	Scd	5.9	−18.7	121	12, 20
NGC 6674	Sb	49.3	−21.6	291	3,9
NGC 6946	Scd	10.1	−21.4	170	11, 17
NGC 7331	Sb	14.9	−21.4	257	12, 14
UGC 2259	Sdm	9.8	−17.0	90	21, 14
UGC 2285	Sc	78.7	−22.8	298	10, 22

Galaxy types, listed in column (2), have been taken from Broeils (1992a) or from the original papers. Distances as given in Broeils (1992a) have been adopted ($H_0 = 75\,{\rm km\,s^{-1}\,Mpc^{-1}}$). Total blue magnitudes have been taken from Broeils (1992a) as well, when available. If not, we used values listed in the original papers. $V_{\rm max}$ is the maximum observed rotation velocity of the galaxy.
Key to the references: 1, Carignan & Freeman (1988); 2, Carignan & Beaulieu (1989); 3, Broeils (1992a); 4, Lake, Schommer & van Gorkom (1990); 5, Puche, Carignan & Wainscoat (1991); 6, Carignan & Puche (1990); 7, Carignan (1985b); 8, Puche, Carignan & Bosma (1990); 9, Broeils & Knapen (1991); 10, Kent (1986); 11, Carignan et al. (1990); 12, Broeils (1992b); 13, Begeman (1987); 14, Kent (1987); 15, Jobin & Carignan (1990); 16, Begeman (1989); 17, Kamphuis (1993); 18, Kent (1984); 19, Côté, Carignan & Sancisi (1991); 20, Wevers (1984); 21, Carignan, Sancisi & van Albada (1988); 22, Roelfsema & Allen (1985); 23, Sicking (1997).

3 THE SAMPLE

The sample used for this study is essentially that of Broeils (1992a), with galaxies characterized by the following:

(i) The H I rotation curve has been measured with the Westerbork Synthesis Radio Telescope or with the Very Large Array.

(ii) The galaxy has a smooth and fairly symmetric velocity field and gas distribution.

(iii) High-precision photometric data are available.

(iv) Inclination and position angle have been derived kinematically, using a tilted ring analysis of the velocity field.

We have included NGC 5371 (Begeman 1987), which was not used by Broeils 'because of its clumpy gas distribution and asymmetric velocity field'. For our purpose the properties of this galaxy are sufficiently regular. We have further added NGC 6946 using data from Kamphuis (1993). NGC 1003 from Broeils' sample could not be used, because the data are not readily available. The selected galaxies are listed in Table 1, together with some of their basic properties. The distances given in this table are based on the values (adopting $H_0 = 75\,\mathrm{km\,s^{-1}\,Mpc^{-1}}$) given in Broeils (1992a). For NGC 5371 and 6946, distances from Begeman (1987) and Carignan et al. (1990) have been used.

The galaxies in Table 1 span a considerable range in Hubble type, from Sab to Irr. Although most galaxies are of type Sc or later, the sample allows for a systematic study of galaxy properties from types Sb to Irr. Note that our sample does not include LSB galaxies.

The light profiles and H I surface density distributions for the galaxies in Table 1 are shown in Fig. 1. Apart from the occasional presence of a bulge, most light profiles are essentially exponential. The H I surface density distributions show a larger variety of shapes, but the maximum surface densities reached in the inner regions are remarkably similar: about $6\,\mathrm{M_\odot\,pc^{-2}}$. Note the larger radial extent of the neutral hydrogen component compared to the light, and the steepening of the H I profile in the outer region for several galaxies. However, for some of the dwarf galaxies the scalelengths of light and H I gas are quite similar.

The H I surface density profiles in Fig. 1 have been derived from 21-cm line synthesis observations. For large galaxies the H I flux in the outer parts may therefore have been underestimated. As a consequence of the missing 'large-scalelength' H I components, rotation curves in Fig. 2 may show a decrease in the outermost parts. Comparison of the total flux with that measured with single-dish telescopes (Rots 1980) shows that the profiles of NGC 55 and 300 may well suffer from this. This may also be true for NGC 3109.

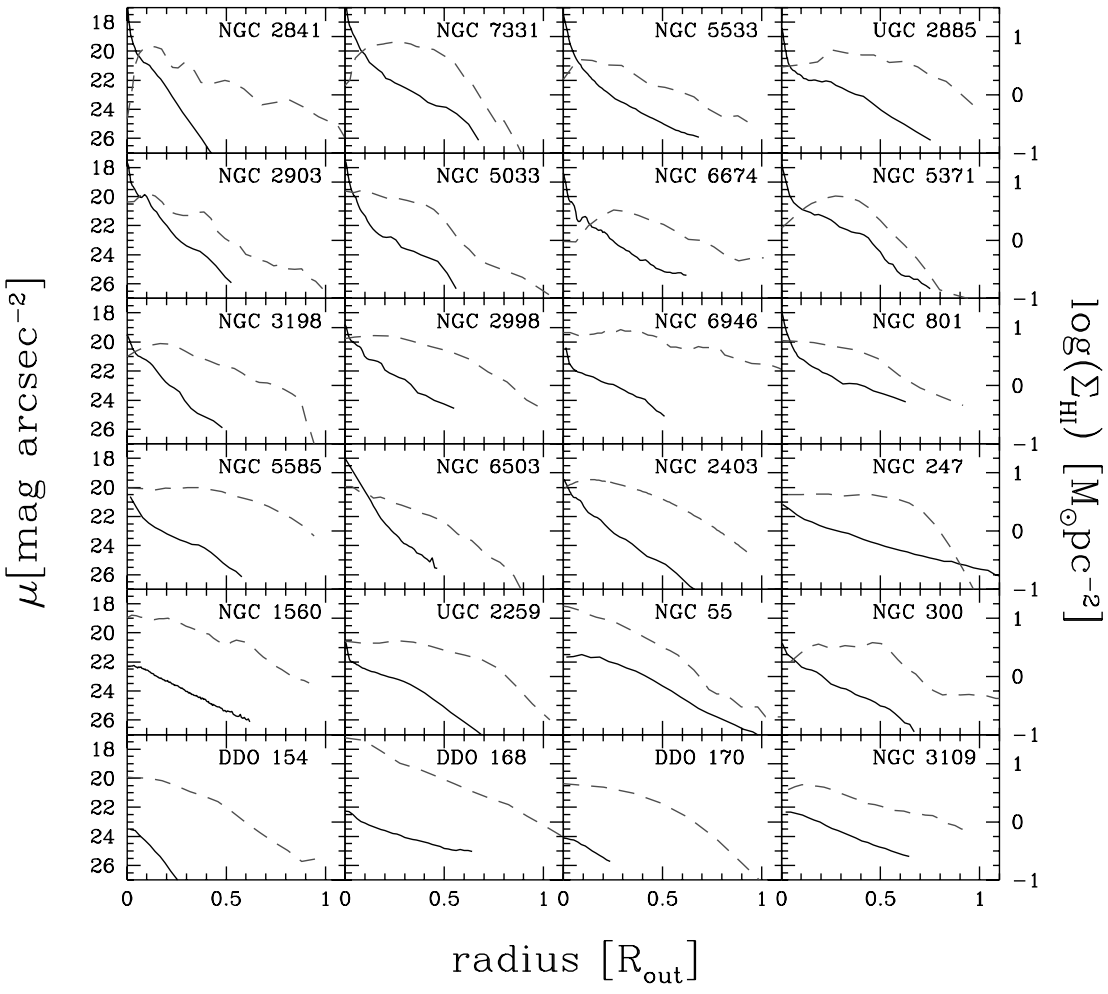

Figure 1. Mosaic of *r*-band surface brightness profiles (solid lines) and H I surface density profiles (dashed lines) of the galaxies in our sample. The profiles are plotted against radius expressed in R_{out}, the outermost point of the rotation curve.

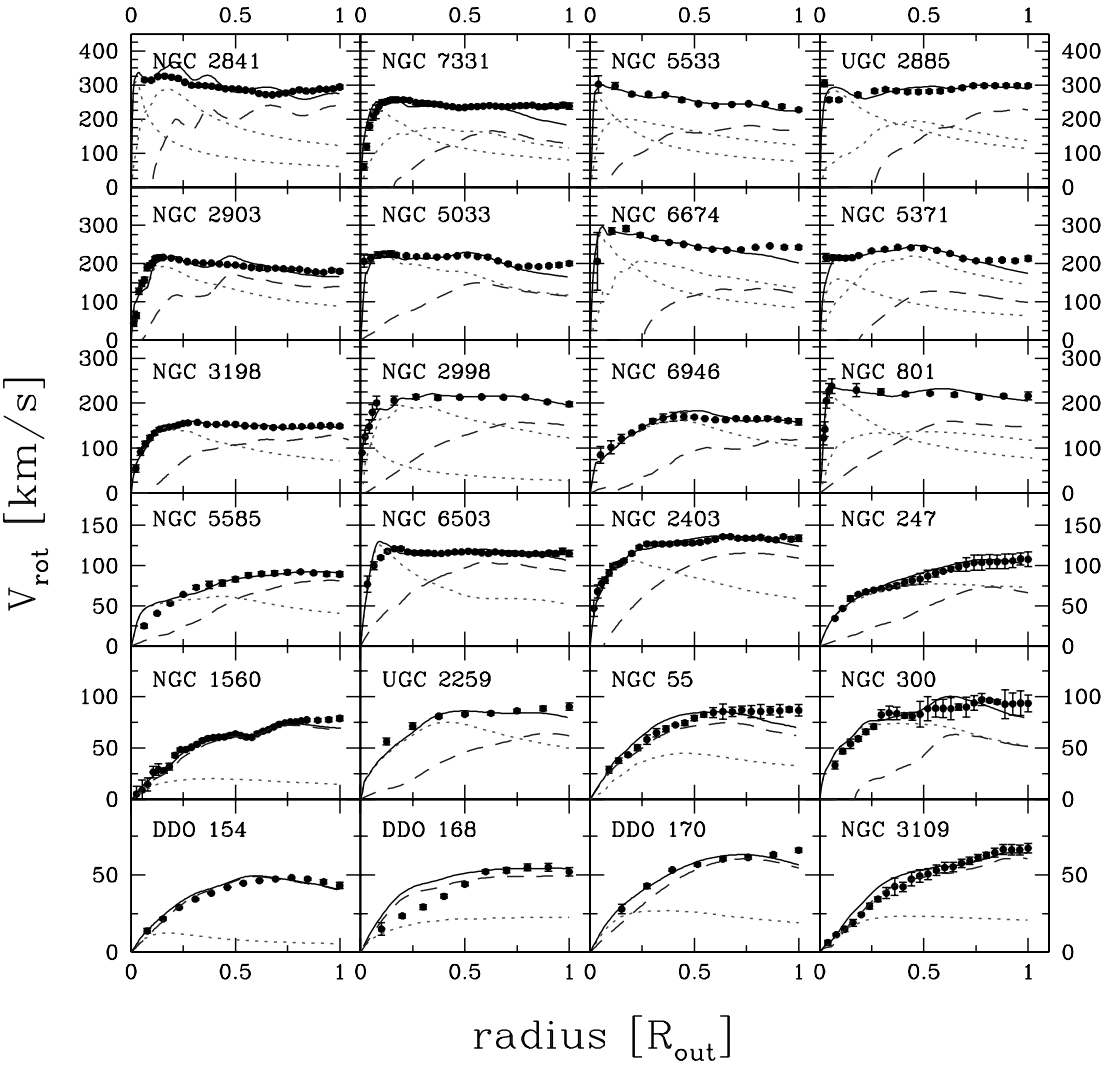

Figure 2. Mosaic of rotation curves. The published rotation curves are the dots with error bars. The model fits to these rotation curves are indicated by the solid lines. The dotted lines denote the disc and, if included, the bulge contribution. The dashed lines correspond to the scaled H I contribution. The curves are plotted against radius expressed in $R_{\rm out}$, the outermost point of the rotation curve. Error bars in the published rotation curves are usually formal errors from the tilted ring model fits. The true uncertainties are probably somewhat larger, perhaps a factor of 2, than the quoted errors.

4 RESULTS OF MASS MODEL FITS

In this section we present and discuss the fits of the adopted mass model to the rotation curves of the 24 galaxies in Table 1. In Table 2 we list the values of the fitted parameters and the inferred masses of the various components.

The models are compared to the observed rotation curves in Fig. 2. The radius is expressed in units of $R_{\rm out}$, the radius of the last measured point of the rotation curve. The circular velocities for the stellar component(s) (dotted) and the scaled H I component (dashed) are also plotted.

We see that most of the 24 rotation curves can be fitted rather well over their full extent by scaling up the H I surface density. The poorer fits can be categorized as follows:

(i) The model curve does not agree with the observed rotation curve in the inner region. This may be due to an incorrect bulge contribution. For dwarf galaxies the inner parts of the rotation curves may be affected by beam smearing, as in the case of NGC 5585 – compare with the optical rotation curve by Blais-Ouellette et al. (1999). In the case of DDO 168 the published rotation curve may be too low in the inner parts and the model rotation curve is in fact consistent with the observations. The fits for the other dwarf galaxies in Table 2 are quite acceptable.

(ii) The model rotation curve shows large wiggles that are not present in the observed rotation curve. This effect is seen for NGC 2841, 2903 and 300. In estimating the contribution of the gas to the rotation velocity, we have used a radial profile that is an azimuthal average of the H I distribution. Features such as spiral arms or blobs of H I, however, may cause bumps in the radial profile. In the model rotation curve strong features will then show up, because the scaling of H I amplifies the irregularities in the H I distribution. Indeed the H I map of NGC 2903 shows clear spiral structure and blobs related to the wiggles. For NGC 2841 and 300 the situation is less clear. The presence of wiggles in the rotation curves shows that the distribution of dark matter cannot be an exact copy of the distribution of H I. At best, the smeared-out distribution of H I is a tracer of dark matter.

(iii) The model rotation curve drops below the observed rotation curve at large radii. Seven galaxies fall in this category (NGC

Table 2. Results of mass model fits.

Name (1)	Type (2)	$(M/L_B)_{\rm disc}$ (3)	$(M/L_B)_{\rm bulge}$ (4)	$\Sigma_{\rm dark}/\Sigma_{\rm H\,I}$ (5)	$M_{\rm disc}$ (6)	$M_{\rm bulge}$ (7)	$M_{\rm H\,I}$ (8)	$M_{\rm tot}$ (9)
DDO 154	Irr	1.0	–	8.0	0.052	–	0.28	2.6
DDO 168	Irr	1.2	–	7.0	0.23	–	0.21	1.9
DDO 170	Sm	3.5	–	9.5	0.34	–	0.45	5.3
NGC 55	Sm	0.5	–	7.0	2.2	–	0.9	9.4
NGC 247	Sd	4.4	–	8.0	11	–	0.8	18
NGC 300	Sd	2.8	–	11.0	5.9	–	0.7	14
NGC 801	Sc	2.8	4.5	9.0	160	72	22	450
NGC 1560	Sd	1.0	–	7.0	0.36	–	0.82	6.9
NGC 2403	Scd	1.8	–	9.5	15	–	3.1	46
NGC 2841	Sb	5.3	3.1	23.0	280	68	16	730
NGC 2903	Sbc	2.7	–	37.0	43	–	2.4	130
NGC 2998	Sc	1.5	5.0	7.0	130	8.5	23	320
NGC 3109	Sm	0.8	–	13.5	0.66	–	0.49	7.8
NGC 3198	Sc	3.9	–	12.5	35	–	5.0	100
NGC 5033	Sbc	5.8	–	12.0	110	–	6.5	190
NGC 5371	Sb	2.9	3.3	8.0	120	60	8.6	260
NGC 5533	Sab	5.0	8.0	16.5	220	96	25	750
NGC 5585	Sd	2.0	–	9.0	3.2	–	1.3	16
NGC 6503	Scd	1.2	–	17.5	5.6	–	1.6	35
NGC 6674	Sb	4.5	7.0	9.0	210	110	30	620
NGC 6946	Scd	1.2	–	4.5	53	–	20	160
NGC 7331	Sb	4.6	1.8	8.0	110	59	11	270
UGC 2259	Sdm	4.0	–	10.0	3.9	–	0.42	8.5
UGC 2885	Sc	1.5	7.5	9.5	270	210	44	940

Mass-to-light ratios in columns (3) and (4) are given in units of $M_\odot/L_{B\odot}$; masses in columns (6), (7), (8) and (9) are given in $10^9\,M_\odot$. Column (9) gives the total mass of the model.

7331, 5033, 6674, 5371, 1560, 55 and 300). In Section 3 we noted that for large galaxies H I flux may be missed in the 21-cm synthesis observations. Obviously this could be a factor contributing to a decline of the H I rotation curve in the outer parts. In the same vein, hydrogen may be partly ionized in the outer regions due to photons of intergalactic origin. This possibility has been discussed for NGC 3198 by Maloney (1993). Irrespective of the presence of molecular gas, the observed H I surface density may therefore not always trace the total gas density in the outer parts.

We conclude from the comparisons in Fig. 2 and the results above that the rotation curves of two-thirds of the galaxies in our sample, spirals and dwarfs alike, can be fitted with a mass model based on the distribution of light and the distribution of H I, provided that the scalefactors $M_\odot/L_{B\odot}$ and $\Sigma_{\rm dark}/\Sigma_{\rm H\,I}$ can be chosen freely. The values we find for the mass-to-light ratios of the stellar component(s) agree well with the values given in Broeils (1992a) and Begeman (1987). From Fig. 2 one sees that many fits are nearly maximum disc fits (van Albada & Sancisi 1986). This is indeed a remarkable property of this type of modelling: scaling of H I to represent the dark component only works in combination with maximal discs. We have verified this by gradually lowering the disc mass. Decreasing the disc mass by more than $\sim$10 per cent below its maximum value results in a substantially smaller core radius of the dark component, and such a dark component can then no longer be represented by a scaled-up H I distribution.

In Fig. 3 the frequency distribution of the scaling factor is shown. It is strongly peaked around a value of approximately 9. Correcting for primordial helium, we find that the dark matter surface density is approximately 6.5 times the gas surface density (i.e. H I + He). As can be seen from Table 2, the H I scalefactor does not change much with galaxy type, although the scatter increases towards earlier types.

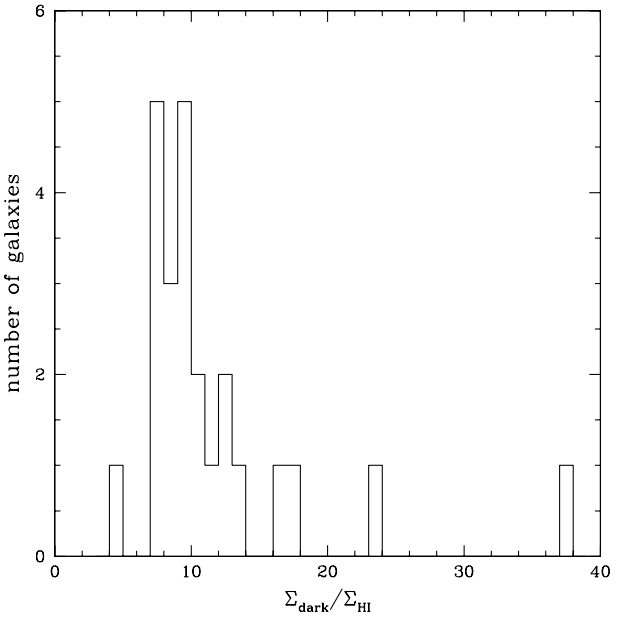

Figure 3. Frequency distribution of the scaling factor $\Sigma_{\rm dark}/\Sigma_{\rm H\,I}$ found for the galaxies in our sample.

Two galaxies, NGC 2841 (23) and NGC 2903 (37), have $\Sigma_{\rm dark}/\Sigma_{\rm H\,I} > 20$. These galaxies are the two most compact ones in the sense that they have small scalelengths in comparison to their maximum rotation velocities; they therefore require a relatively massive dark halo. Their H I surface densities do not differ much from those of other galaxies and this results in an H I scalefactor that is above average.

5 DISCUSSION

As shown above, in general the distribution of H I mimics the distribution of dark matter remarkably well, provided the contribution of the disc to the rotation curve is close to maximal. We now examine more closely which property, or properties, of the H I layer in galaxies play(s) a role in this.

5.1 Bias against small H I scalelength

The rotation curves of the galaxies in our sample extend to well beyond the radius of 2.2 scalelengths where the rotation curve of the luminous component reaches its maximum. For a good match, we therefore require a rotation curve for the H I component rising to well beyond $2.2h_{\rm stars}$, in order to compensate for the decline of the rotation curve of the stars. Put differently, the radial 'scalelength' of the H I distribution must be large, about 0.4 times the outer radius of the H I disc, $R_{\rm out}$, or even larger. For the galaxies in our sample we find an average $h_{\rm H\,I} \simeq 0.33R_{\rm out}$, only barely enough for H I scaling to work. Fig. 1 shows that for most galaxies the H I surface density profiles curve downwards with increasing radius. This is why for several galaxies scaling of H I gives a poor fit in the outer parts, with the model curve falling below the observed rotation curve (see e.g. NGC 7331 and 5371). Apparently, with the present 21-cm line sensitivity we may be reaching the border of the region where scaling of atomic hydrogen to fit the rotation curve works. Extension of the rapidly declining H I surface density profiles to larger radii would result in progressively poorer fits.

It is worth noting that our selection in favour of a large radial extent in H I excludes galaxies with small H I scalelengths, for the following reason. The H I surface density in the inner region of spiral galaxies, leaving aside a possible central depression, varies only by a modest amount from galaxy to galaxy (Broeils 1992a; Rhee 1996; and Fig. 1). In the mean for our sample $\Sigma_{\rm H\,I}(0) \simeq 6\,{\rm M}_\odot\,{\rm pc}^{-2}$. The smallest H I surface densities measured in the outer regions are set by the sensitivity of the observations. For our sample typically $\Sigma_{\rm H\,I}(R_{\rm out}) \simeq 0.3\,{\rm M}_\odot\,{\rm pc}^{-2}$. The corresponding range in $\Sigma_{\rm H\,I}$ is therefore about a factor of 20 for most galaxies in our sample, corresponding to three scalelengths for an exponential distribution. As a result our sample is biased against galaxies with $R_{\rm out}/h_{\rm H\,I}$ substantially larger than 3. Obviously, for such galaxies scaling of H I to fit the rotation curve does not work.

5.2 The H I scalefactor

Above we have shown that the success of our model fits is related to rather specific properties of the H I distributions for the galaxies in our sample. Could a selection effect also be responsible for the small range in the scalefactor seen in Fig. 3? Below we shall argue that this is unlikely.

Let us assume that the mass distribution in a galaxy can be represented by two exponential discs: one for the stars, and one for the dark matter. The maximum rotation velocity of an exponential disc is proportional to the product of the scalelength and the central surface density. One observes a more or less flat rotation curve when the maximum velocities of both discs are similar, i.e. when

$$\Sigma_{\rm stars}(0)h_{\rm stars} \approx \Sigma_{\rm dark}(0)h_{\rm dark}, \tag{4}$$

where $\Sigma_{\rm stars}(0)$ and $\Sigma_{\rm dark}(0)$ are the central surface densities of respectively the stellar disc and the dark halo, and where $h_{\rm stars}$ and $h_{\rm dark}$ indicate their scalelengths. This equation is a description of the disc–halo conspiracy (van Albada & Sancisi 1986).

If we assume that the surface density profile of the dark matter is a scaled version of the H I surface density, we can write for the scalefactor f:

$$f = \frac{\Sigma_{\rm dark}(R)}{\Sigma_{\rm H\,I}(R)} \approx \frac{\Sigma_{\rm stars}(0)}{\Sigma_{\rm H\,I}(0)}\frac{h_{\rm stars}}{h_{\rm dark}}, \tag{5}$$

where $\Sigma_{\rm H\,I}(0)$ is a measure of the maximum H I surface density, ignoring a possible central depression. The small spread in the scalefactor f therefore implies a coupling of the scalelengths of stars and dark matter, as well as a coupling of the surface mass densities of stars and H I.

As mentioned above, the maximum surface density of the H I disc of high surface brightness galaxies does not vary much from galaxy to galaxy. Similarly, for luminous spiral galaxies the central surface brightness of the disc is remarkably constant (Freeman 1970). Assuming some constant value for the mass-to-light ratio, this would result in a fairly small variation in the central surface density of the stellar disc. Thus, the spread in the first factor in equation (5) may well be small. This suggests that, if the ratio of scalelengths of the dark disc and the stellar disc were approximately constant, then the scalefactor f would be more or less constant. We note that, when calculating total surface densities from observed rotation curves, we indeed found a more or less exponential surface density profile in the outer parts. The scalelength of this profile was in many cases about 4–5 times the optical scalelength. Thus for the HSB galaxies in our sample, there appears to be a coupling between the linear scales of the disc and the dark halo. Similar results were found by Sackett (1997). Consequently, the expected spread in f is small for HSB galaxies.

Our sample also includes several dwarf galaxies, with central surface brightnesses lower than those of the more luminous galaxies. Their H I surface densities are comparable to the larger galaxies however. Although we do not know how the stellar M/L values of dwarfs and more luminous galaxies differ, it seems unlikely that equation (5) would apply. The similarity of the scalefactor f for dwarfs to that of the more luminous galaxies therefore seems a significant result that cannot easily be explained in terms of a selection effect in our sample.

Swaters (1999) has applied H I scaling to a sample of 35 late-type dwarf galaxies. With one or two exceptions he finds excellent fits. Here too discrepancies, if any, occur mainly in the outermost regions. The required scaling factors for H I show a considerable spread, with a peak between 3 and 6. In the mean they are about a factor of 2 smaller than the scaling factors found above.

6 SUMMARY AND CONCLUSIONS

We have fitted mass models to the observed rotation curves of 24 galaxies under the assumption that the dark matter surface density is proportional to the H I surface density. For about two-thirds of

the galaxies we obtain good fits to the data. After correction for primordial helium the required scaling factor is about 7. The main discrepancies occur at large radii, with the fitted rotation curves falling below the observed ones. This results from a fairly rapid decline of the H I surface density in the outermost regions.

For the H I data used here, the radial density profiles of H I typically extend to about three scalelengths, i.e. close to or just beyond the radius where the rotation curve of the H I component is expected to decline. The good fits are therefore somewhat coincidental. More sensitive H I observations would reach the declining part of the rotation curve of the H I component for several galaxies in our sample (provided the H I surface density remains exponential further out). If the observed circular velocity of the galaxy remains constant with radius, it would then no longer be possible to fit such a flat rotation curve with a scaled-up distribution of H I. Furthermore, in several galaxies scaling up of H I leads to rotation curves with wiggles, and in some galaxies not included in this paper the neutral hydrogen density drops rather abruptly around the optical radius.

Therefore, in many cases, there seems to be little or no relation between H I and dark matter. Note, however, that for a number of reasons (ionization by the intergalactic radiation field, presence of molecular gas and missing H I flux) the observed H I densities may be lower than the actual gas densities. Because of these complications and the selection effects sketched above, it is not possible to conclude here that there is a real coupling between H I and dark matter in spiral galaxies.

ACKNOWLEDGMENTS

We thank Kor Begeman, Adrick Broeils and Floris Sicking for kindly providing their data.

REFERENCES

Begeman K. G., 1987, PhD thesis, Univ. Groningen
Begeman K. G., 1989, A&A, 223, 47
Blais-Ouellette S., Carignan C., Amram P., Côté S., 1999, AJ, 118, 2123
Bosma A., 1978, PhD thesis, Univ. Groningen
Bosma A., 1981, AJ, 86, 1825
Broeils A. H., 1992a, PhD thesis, Univ. Groningen
Broeils A. H., 1992b, A&A, 256, 19
Broeils A. H., Knapen J. H., 1991, A&AS, 91, 469
Carignan C., 1985a, ApJ, 299, 59
Carignan C., 1985b, ApJS, 58, 107
Carignan C., Beaulieu S., 1989, ApJ, 347, 760
Carignan C., Freeman K. C., 1988, ApJ, 332, L33
Carignan C., Puche D., 1990, AJ, 100, 641
Carignan C., Sancisi R., van Albada T. S., 1988, AJ, 95, 37
Carignan C., Charbonneau P., Boulanger F., Viallefond F., 1990, A&A, 234, 43
Côté S., Carignan C., Sancisi R., 1991, AJ, 102, 904
Cuddeford P., 1993, MNRAS, 262, 1076
Freeman K. C., 1970, ApJ, 160, 811
Jobin M., Carignan C., 1990, AJ, 100, 648
Kamphuis J. J., 1993, PhD thesis, Univ. Groningen
Kent S. M., 1984, ApJS, 56, 105
Kent S. M., 1986, AJ, 91, 1301
Kent S. M., 1987, AJ, 93, 816
Lake G., Schommer R. A., van Gorkom J. H., 1990, AJ, 99, 547
Maloney P., 1993, ApJ, 414, 41
Pfenniger D., Combes F., Martinet L., 1994a, A&A, 285, 79
Pfenniger D., Combes F., Martinet L., 1994b, A&A, 295, 94
Puche D., Carignan C., Bosma A., 1990, AJ, 100, 1468
Puche D., Carignan C., Wainscoat R. J., 1991, AJ, 101, 447
Roberts M. S., Whitehurst R. N., 1975, ApJ, 201, 327
Rhee M.-Y., 1996, PhD thesis, Univ. Groningen
Roelfsema P. R., Allen R. J., 1985, A&A, 146, 213
Rots A. H., 1980, A&AS, 41, 189
Rubin V. C., Thonnard N., Ford W. K., Jr, 1978, ApJ, 225, L107
Sackett P. D., 1997, PASA, 14, 11
Shostak G. S., 1973, A&A, 24, 411
Sicking F. J., 1997, PhD thesis, Univ. Groningen
Swaters R., 1999, PhD thesis, Univ. Groningen
van Albada T. S., Sancisi R., 1986, Phil. Trans. R. Soc., London, A320, 447,
van der Kruit P. C., Searle L., 1981a, A&A, 95, 105
van der Kruit P. C., Searle L., 1981b, A&A, 95, 116
Wevers B.H.M.R., 1984, PhD thesis, Univ. Groningen

This paper has been typeset from a TEX/LATEX file prepared by the author.